# *Ventral Prostate Predominant 1*, A Novel Mouse Gene Expressed Exclusively in the Prostate

Judith A. Wubah,[1] Carolyn M. Fischer,[1] Laura N. Rolfzen,[1] May Khalili,[1] Jason Kang,[2] Jeffrey E. Green,[2] and Charles J. Bieberich[1]*

[1]*Department of Biological Sciences, University of Maryland, Baltimore County, Baltimore, Maryland*
[2]*Laboratory of Cell Regulation and Carcinogenesis, National Cancer Institute, Bethesda, Maryland*

**BACKGROUND.** Despite the region-specific nature of human prostate disease, there is a paucity of information regarding the molecular basis of prostate regionalization and patterning. To elucidate genetic mechanisms that underlie prostate growth and development, we investigated differential gene expression in mouse prostate lobes.
**METHODS.** mRNA differential display analysis was used to identify differentially expressed genes during development of ventral, anterior, and dorsolateral prostate lobes. Differential gene expression was confirmed by Northern blot analysis and RT-PCR.
**RESULTS.** A novel gene, *Ventral prostate predominant1* (*Vpp1*) was identified. *Vpp1* mRNA was evident in all lobes but accumulated predominantly in the ventral prostate, and was detected on postnatal day 7 through adulthood exclusively in the prostate gland. The steady-state level of *Vpp1* mRNA decreased markedly in response to castration, suggesting androgen regulation of *Vpp1* expression. Analysis of TRAMP tumors demonstrated a dramatic decrease in the level of *Vpp1* mRNA.
**CONCLUSIONS.** The spatial distribution and early postnatal onset of *Vpp1* expression is consistent with a role for this gene in prostate regionalization. The absolute prostate specificity of *Vpp1* expression may allow this gene to serve as a paradigm to study the molecular basis of gene expression that is restricted exclusively to the prostate gland. *Prostate 51: 21–29, 2002.*


*KEY WORDS:* **prostate-unique; development; androgen regulation; prostate lobes; TRAMP**

## INTRODUCTION

The prostate gland develops late in gestation in response to inductive interactions between the prostatic mesenchyme and the urogenital sinus epithelium [1,2]. Signaling events initiate a process of epithelial invagination that results in the formation of ducts around the circumference of the prostatic urethra. These ducts subsequently undergo a process of branching morphogenesis that ultimately yields a distinct lobular morphology in rodents and a zonal anatomy in humans. The human prostate initially develops with spatially distinct lobes; however, as development proceeds, boundaries between lobes become impossible to distinguish [3]. The gross architecture of the adult human prostate is subsequently referred to in terms of the transition, central, and peripheral zones [3]. Although the functional significance of the lobular and zonal architecture is not well defined, the regional preference of human prostate disease underscores the need to understand the

The authors acknowledge that they have no affiliations to any organizations or corporations that may be considered a conflict of interest in the subject matter discussed.

Grant sponsor: NIDDK (to C.J.B.); Grant number: RO1DK54067; Grant sponsor: NIDDK (to J.A.W.); Grant number: F22DK10094-01.

*Correspondence to: Charles J. Bieberich, PhD, Department of Biological Sciences, University of Maryland, Baltimore County, Baltimore, Maryland, 21250. E-mail: bieberic@umbc.edu

Received 30 October 2001; Accepted 26 November 2001

DOI 10.1002/pros.10060

processes that initiate and maintain these distinct morphological areas.

A striking feature of prostate biology is the fact that prostate cancer and benign prostatic hyperplasia (BPH), two age-related proliferative diseases, are typically confined to separate areas of the gland. The overwhelming majority of prostate cancer occurs in the peripheral zone, while BPH occurs almost exclusively in the transition zone [4,5]. The central zone is rarely affected by either prostate cancer or BPH.

Despite the region-specific nature of prostate disease, the molecular basis of prostate regionalization has not been systematically addressed. The lack of information regarding pattern formation in the prostate stems from the fact that the genetic pathways underlying normal prostate growth and differentiation remain to be elucidated. The difficulties in using human material to identify factors that may mediate regional differences in early prostate differentiation and to perform genetic analyses of their function are axiomatic. Hence, the systematic elucidation of the cellular and molecular mechanisms that underlie initiation and maintenance of normal prostate growth will likely rely on the use of animal models. Although rodents typically do not develop spontaneous proliferative pathologies of the prostate, they have historically been extensively used to study prostate biology. In mice and rats, the ventral, anterior (coagulating glands), lateral, and dorsal lobes remain as spatially distinct lobes throughout life. Although homologous relationships between regions of rodent and human prostates have been suggested based on a classical descriptive comparison of ductal openings [6], no molecular markers that could verify this hypothesis have been reported. Since murine models are likely to continue to serve as paradigms for human prostate disease, it is clearly important to determine homologous relationships between human zones and rodent lobes.

The recognition that most diseases in the adult human prostate are a result of disorders in proliferation and differentiation prompted us to search for genes that are differentially expressed among prostate lobes during growth and differentiation. We employed an mRNA differential display approach to analyze gene expression in the developing mouse prostate during the process of branching morphogenesis and prior to the initiation of major secretory protein production. We report here a novel gene, designated *Vpp1*, that is expressed exclusively in the prostate and predominantly in the ventral prostate. *Vpp1* expression decreases after castration and is markedly downregulated in transgenic adenocarcinoma of mouse prostate (TRAMP) tumors. The unique expression pattern of *Vpp1* may allow this gene to serve as a model to elucidate the molecular basis of differential gene expression in normal and diseased prostates.

## MATERIALS AND METHODS

### Animals

Pregnant CD-1 mice from Charles River Breeding Laboratories (Wilmington, MA) were housed in a temperature-controlled room on a 12 hr light/dark schedule. Mouse chow and water were provided ad libitum. Day of birth was designated postnatal day 1 (PND1) and animals were euthanized on PND13 by carbon dioxide asphyxiation. Orchiectomy of adult mice was performed as described for rats [7].

### mRNA Differential Display

Differential display reverse transcription-polymerase chain reaction (DD-RTPCR) was performed using the Hieroglyph mRNA profile kit (Beckman Coulter, Foster City, CA). Microdissection of PND13 prostates into ventral, anterior, and dorsolateral lobes was performed as described [8]. Total RNA was extracted using an RNeasy kit (Qiagen, Valencia, CA) followed by treatment with RNase-free DNase I (Ambion, Austin, TX). Two hundred nanograms of total RNA from individual pooled lobes were reverse transcribed with 1 of 12 anchored primers (5′T7(dT12) CA3′) using the following conditions, 42°C for 5 min, 50°C for 50 min, 70°C for 15 min. Polymerase chain reaction amplifications of first strand cDNAs were performed in the presence of dNTP mix (250 μM each), the same anchored primer used for RT (2 μM), arbitrary primer number 5, 5′-ACAATTTCACACAGGAGCTAGCATGG (2 μM, Beckman Coulter), and 0.25 μl of $^{33}$P-dATP (3000 Ci/mmole; New England Nuclear, Boston, MA) according to manufacturer's recommendations. Thermal cycling was performed in an MJ Research PTC 200 cycler (Waltham, MA) under the following conditions: 95°C for 2 min; 4 cycles of 92°C for 15 sec, 50°C for 30 sec, 72°C for 2 min; 30 cycles of 92°C for 15 sec, 60°C for 30 sec, 72°C for 2 min; 72°C for 7 min; 4°C, hold. Three and one half microliters of denatured PCR products were loaded onto a denaturing 4.5% polyacrylamide gel and electrophoresed in a GenomyxLR DNA sequencer (Beckman Coulter). Dried gels were exposed to BioMax-MR film (Eastman Kodak, Rochester, NY) for 3–5 days. In all cases, a 100 bp DNA ladder (Life Technologies, Gaithersburg, MD) was labeled with $^{33}$P and electrophoresed in parallel with the DD-RTPCR samples to provide accurate estimation of band size. The primer combination generated several hundred bands ranging from 500 bp to over 2 kb in size. Differentially displayed bands (e.g., *Vpp1* and others) were identified, excised,

and reamplified using the Expand High Fidelity PCR kit (Roche Biochemicals, Indianapolis, IN) following manufacturer's instructions. The reamplification primers were T7 promoter 5′-GTAATACGACTCACTATAGGGC-3′ and M13 reverse (-48) 5′-AGCGGATAACAATTTCACACAGGA-3′. Reaction products were analyzed on 1% agarose gels and amplified products were purified using Princeton Separation columns (Adelphia, NJ). The purified products were subcloned into pCRII-TOPO vector (Invitrogen, Carlsbad, CA) and probes were generated from representative plasmid DNA.

### Northern Blot Analysis

Total RNA aliquots of 3 μg (PND13) or 5 μg (adult) prostate, seminal vesicle, and various tissues were separated on 1% glyoxal/dimethylsulfoxide/agarose gels (Ambion). RNA was transferred onto NytranN membrane (Schleicher and Schuell, Keene, NH). Following manufacturer's recommendations, 50 ng of linearized plasmid DNA were used to generate probes using the Strip-EZ PCR kit (Ambion). The filters were prehybridized in ULTRAhyb$^{TM}$ solution (Ambion) for 1 hr at 42°C and hybridized overnight at 42°C in the same solution containing a final probe concentration of $10^6$ cpm/ml. Filters were washed twice at 42°C in Low Stringency Buffer (Ambion) for 5 min each followed by two washes in High Stringency Buffer (Ambion) for 15 min each. Filters were exposed to X-101 film (Kodak) for up to 4 hr at −70°C depending on signal intensity. For hybridization with control probes, blots were stripped using Strip-EZ reagents (Ambion) and probed with β-actin or glyceraldehyde-3-phosphate dehydrogenase (GAPDH). The level of mRNA in each tissue was determined by phosphorimaging of Northern blots, using β-actin or GAPDH mRNA levels in the same samples for normalization.

### Sequence Analyses

*Vpp1* sequence data was compared to sequences in GenBank using the BLASTn algorithm on the non-redundant or dbEST databases. The sequence did not produce any matches in either database and was designated a novel transcript. Using the deduced amino acid sequence, the PSORT algorithm [9] was utilized to analyze the sequence for the presence of signal peptides, transmembrane domains and to predict protein subcellular localization.

### 5′/3′ Rapid Amplification of cDNA Ends (RACE)

For 5′ RACE, a gene-specific reverse transcription primer, 5′-CACAAGCCTTGGGTTTGTCT-3′, was used to generate cDNA from 2 μg of total prostate RNA. PCR was performed using 5′-CGACUGGAGCACGAGGACACUGA-3′, and GeneRacer (Invitrogen) kit components according to the manufacturer's recommendations using the following cycling conditions: 94°C for 2 min; 10 cycles of 94°C for 15 sec, 55°C for 30 sec, 72°C for 40 sec; 25 cycles of 94°C for 15 sec, 55°C for 30 sec, 72°C for 40 sec + cycle elongation of 20 sec; 72°C for 7 min; 4°C, hold. For 3′ RACE, the GeneRacer Oligo (dT)18 primer was used for first strand cDNA synthesis followed by PCR using 5′-CCTCGATCCCTGTGGCTGCTGTCTGT-3′/5′-GCTGTCAACGATACGCTACGTAACG-3′ primer pair. Specific RACE products were subcloned into pCRII-TOPO vector (Invitrogen) and sequenced.

### RT-PCR

First strand cDNA was prepared using total RNA and the RETROscript kit (Ambion). Briefly, 12 μl of template and random decamers primer mixture containing 200 ng of total RNA were incubated at 85°C for 3 min. Reverse transcription buffer, dNTP mix, and reverse transcriptase were added to a final volume of 20 μl and RT was carried out at 55°C for 1 hr. Samples were heated to 92°C for 10 min to inactivate the RT enzyme. A gene-specific primer pair (5′-GTGTTGTGATGCCAGGTCAC-3′)/(5′-ACATTTGGGATGGTTCAGGA-3′) was used to assess expression using the same cycling profile described above for the RACE reactions. Controls for RT-PCR assays included PCR amplification of the RNA samples without reverse transcription or RNA template. In addition, amplification of a highly conserved region of the constitutively expressed housekeeping gene, rat insulinoma gene (*rig*), which encodes a ribosomal subunit protein [10,11], served as a positive control.

### In Situ Hybridization

To generate a *Vpp1* antisense probe for in situ hybridization, a plasmid consisting of bases 82–666 of the *Vpp1* cDNA cloned into pCRII-TOPO vector (Invitrogen) was linearized with Apa I and digoxigenin-(DIG) labeled RNA was generated using T7 RNA polymerase. As a control for non-specific hybridization, a DIG-labeled antisense probe encoding a 600-base portion of the *Escherichia coli* lacZ gene was hybridized to parallel sections. Hybridization and washing were performed as described [12], and for color development, nitroblue tetrazolium chloride/5-bromo-4-chloro-3-indolylphosphate p-toluidine (NBT/BCIP) was used as a substrate for alkaline phosphatase. Images were captured using a Nikon DMX1200 digital camera.

## RESULTS

### Identification, Cloning, and Sequence Analysis of *Vpp1*

Differential display analysis revealed a 584 bp cDNA fragment in PND13 ventral and dorsolateral lobes. Analysis of the longest open reading frame (ORF) predicted a polypeptide consisting of 135 amino acid residues. The mouse *Vpp1* cDNA and its deduced amino acid sequence are shown in Figure 1. Analysis of 5′ and 3′ RACE products allowed prediction of a full-length sequence of 798 bp. The 5′ untranslated region (UTR) was 87 bp in length, followed by an ORF of 408 bp, a termination codon, and a 303 bp 3′ UTR. Three in-frame stop codons were present upstream of the presumptive translation initiation site. This site, AagATGG, conforms to the Kozak consensus motif, RNNatgY in an adequate context [13]. A polyadenylation consensus sequence was observed 267 bases downstream of the stop codon in the 3′ UTR. BLAST analysis of GenBank DNA and protein databases detected no significant homologies to any deposited sequence. Analysis using the PSORT algorithm [9] predicted Vpp1 to be an extracellular protein with a cleavable secretory signal peptide (Fig. 1).

### *Vpp1* Expression in PND13 and Adult Prostates

Northern blot analysis was used to determine the expression profile of *Vpp1* in PND13 prostate lobes (Fig. 2). The *Vpp1* cDNA probe detected a single transcript in prostate RNA, with the highest expression in the ventral lobe. The steady-state level of *Vpp1* mRNA accumulation in the dorsolateral lobe was consistently 8-fold lower than that observed in the ventral lobe. The lowest level of *Vpp1* mRNA accumulation occurred in the anterior lobe, which was 11-fold lower than in the ventral. This distribution of expression is consistent with the initial DD-RTPCR analysis, but demonstrates that the level of expression in the anterior lobe was below the threshold for detection in that assay. The ventral lobe predominance of *Vpp1* expression was also maintained in adult animals. In adult mice, the dorsal and lateral components of the dorsolateral can be readily separated. As in PND13 prostates, the highest steady-state level of *Vpp1* mRNA was observed in the ventral lobe, in a decreasing order of ventral > lateral > dorsal > anterior.

### *Vpp1* Transcript Expression is Unique to the Prostate

To determine the tissue distribution of *Vpp1* mRNA in the urogenital system of both male and female mice, total RNA was extracted from ampullary gland, bladder, bulbourethral gland, seminal vesicle, testis, urethra, cervix, ovary, oviduct, uterus, and vagina, and was screened by Northern blot analysis (Fig. 3 and data not shown). The *Vpp1* mRNA was not detected in any other urogenital tissue, including the bulbourethral gland, which, like the prostate, is an endodermally derived secretory organ that develops from the urogenital sinus. To determine the total body distribution of *Vpp1* mRNA, a panel of 20 normal adult tissues was screened by Northern blot analysis. Remarkably, no accumulation of *Vpp1* mRNA was observed in any other tissue, including mammary gland (Fig. 3 and data not shown). These data demonstrate that *Vpp1* mRNA expression is unique to the prostate.

### Developmental Expression of *Vpp1*

To ascertain the temporal onset of *Vpp1* expression, RNA from PND7, PND10, and PND13 prostate lobes were screened by Northern blot analysis. *Vpp1* expression was readily detected in PND10 and PND13 ventral lobes, but was not observed in PND7 RNA (Fig. 4A). To confirm these results and to extend the analysis to an earlier developmental stage, RNA from PND1 total prostate, as well as PND7 and PND10 ventral lobes, was analyzed by RT-PCR. As shown in Figure 4B, expression was detected on PND7 but not on PND1. These data demonstrate that *Vpp1* transcription is initiated in the first week of postnatal life during a period of robust branching morphogenesis.

### Effect of Castration on Expression of *Vpp1*

To determine whether *Vpp1* was androgen-regulated, RNA was extracted from adult prostates harvested from pools of two mice at various time points after castration, but preceding onset of an atrophic state. Northern blot analysis revealed that 24 hr after castration, the *Vpp1* mRNA level had decreased 2-fold (Fig. 5). The steady-state level of *Vpp1* mRNA continued to decline, and by 14 days post-castration, was decreased nearly 10-fold (Fig. 5). To ascertain whether the decrease in *Vpp1* mRNA in response to castration was lobe-dependent, the experiment was repeated using RNA extracted from individual lobes after castration. The *Vpp1* mRNA level decreased in all lobes in response to castration (data not shown).

### *Vpp1* Expression in TRAMP Tumors

Prostate tumors were dissected from six TRAMP mice that ranged in age from 6 to 11 months. Northern blot analysis showed a 150-fold decrease in *Vpp1* mRNA in two tumors and no expression in the other four analyzed (Fig. 6 and data not shown).

```
CATGGACTGAAGGAGTAGAAAGTTTCCTGTAAGGCATTCTGATTGCCAGCC                51
AGGGGTGGAAACATTTGTTGGTATCACTGAGCTAAG ATG GTG TTA CCT CGA          102
                                      M   V   L   P   R            5
TCC CTG TGG CTG CTG TCT GTC TGT CTT CTG TCC TGG TGT TGT GAT GCC AGG 153
S   L   W   L   L   S   V   C   L   L   S   W   C↑C   D   A   R    22
TCA CTA GGT CCT CAA GAT CTA CAG CTA GAA TCA TGG CAA ATA ACT TTT GTG 204
S   L   G   P   Q   D   L   Q   L   E   S   W   Q   I   T   F   V   39
TTC TTG CAT CTG AAA GGA GAA ACA ATA AGT ATG GAT GAC ATT GAA GTG ATG 255
F   L   H   L   K   G   E   T   I   S   M   D   D   I   E   V   M   56
TTT CAA ATG AAT AAA GCT GGA GCT TAT GTC CCA TCT GTT GAG ACT GAG AAG 306
F   Q   M   N   K   A   G   A   Y   V   P   S   V   E   T   E   K   73
GCT GTG ATG GAG GAT ATG GAT AAC AAA GCC TTG TAT GTC AGC TCA CAT GCA 357
A   V   M   E   D   M   D   N   K   A   L   Y   V   S   S   H   A   90
TTT AAG ATT CTC CCT AAG CAG CCT AAG TTG AGA CAT GGC CAC ACT GAT TTT 408
F   K   I   L   P   K   Q   P   K   L   R   H   G   H   T   D   F  107
AAA TTT CCT GAA CCA TCC CAA ATG TGG AAG GTA TTG ATG AAC GAT GAC TCT 459
K   F   P   E   P   S   Q   M   W   K   V   L   M   N   D   D   S  124
ACC CGC TAC AAA TTG AAA TTT TGG CAA AGA ACT TGA GAGAGTCCTGAAGAA    510
T   R   Y   K   L   K   F   W   Q   R   T   *                     135
ACTTGTCCCAATATGGGATATTCCAGGGAATGGTCATAAGACAAACCCAAG               561
GCTTGTGTAAATATTGTGAAGACAGCAATACTTTGCATGCATTTTGAACTA               612
TGAAGACACAACAAAACTGAAAAAGAACAACCCTGCTTACAAAGTAGAGTT               663
TAGTCTCCTGCTACTTAACATAGCCGCTTTCTTTCTCTGTCCTCATTTGGG               714
AAAATTTCCTAATCTGTAAGACAGGCATGCTCACTTAGTGTAAGCTCTTCT               765
CAGGTTCTCTGAaataaaCTTAACTGCACTTTG                                 798
```

**Fig. 1.** Characterization of full-length *Vppl* cDNA sequence. Nucleotide and predicted amino acid sequences of *Vppl*. The potential initiation methionine codon and translational stop codon are indicated in bold. The secretory signal peptide sequence is underlined. An arrow indicates possible cleavage site and the putative polyadenylation signal is displayed in small case text. The GenBank accession number for *Vppl* is AY077734.

### Distribution of *Vppl* Within the Prostate

In situ hybridization to histological sections was performed to characterize the cellular distribution of *Vpp1* within the prostate. Analysis of serial sections hybridized with *Vpp1* antisense and control probes showed signal with only the *Vpp1* antisense probe, confirming the specificity of hybridization (Fig. 7). Expression of *Vpp1* was detected exclusively over the epithelial cells lining the ducts (Fig. 7). No hybridization signal was detected in stromal cells. The difference in signal between control and antisense probes demonstrated the specificity of the antisense probe.

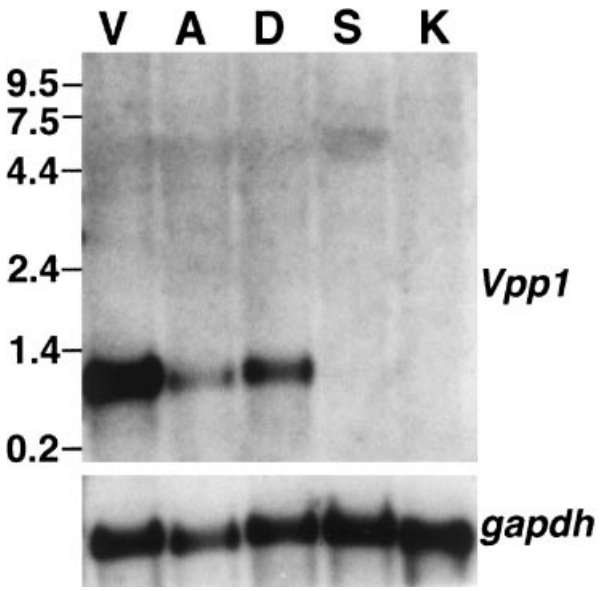


**Fig. 2.** Northern blot analysis of *Vppl* expression in PNDI3 prostate lobes. (Top) Total RNA (3 μg/lane) was electrophoresed and hybridized with *Vppl* cDNA probe. V, ventral prostate; A, anterior prostate; D, dorsolateral prostate; S, seminal vesicle; K, kidney. (Bottom) Hybridization of the same Northern filter with a GAPDH probe.

## DISCUSSION

With a long-term view towards understanding the molecular basis of regionalization and proliferative disorders of the prostate, we have initiated a systematic analysis of differential gene expression within developing prostate lobes. This search identified a novel gene, *Vpp1*, which is expressed predominantly

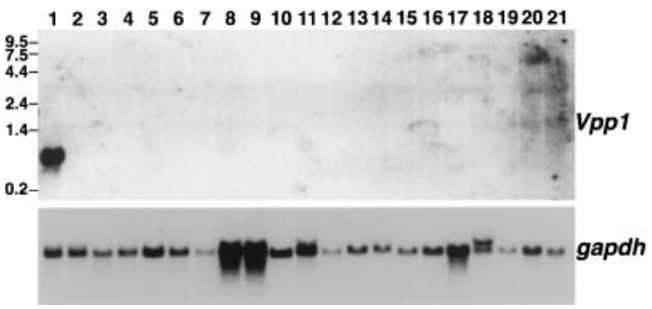


**Fig. 3.** Profile expression of *Vppl* in adult tissues. (Top) Five micrograms of total RNA were transferred to a membrane and hybridized with *Vppl* cDNA probe. **Lane 1**, total prostate; **Lane 2**, bladder; **Lane 3**, seminal vesicle; **Lane 4**, testis; **Lane 5**, urethra; **Lane 6**, lachrymal gland; **Lane 7**, preputial gland; **Lane 8**, salivary gland; **Lane 9**, liver; **Lane 10**, lung; **Lane 11**, brain; **Lane 12**, heart; **Lane 13**, skeletal muscle; **Lane 14**, smooth muscle; **Lane 15**, spleen; **Lane 16**, thymus; **Lane 17**, kidney; **Lane 18**, stomach; **Lane 19**, small intestine; **Lane20**, large intestine; **Lane 21**, rectum. (Bottom) Hybridization of the same blot with a GAPDH probe.

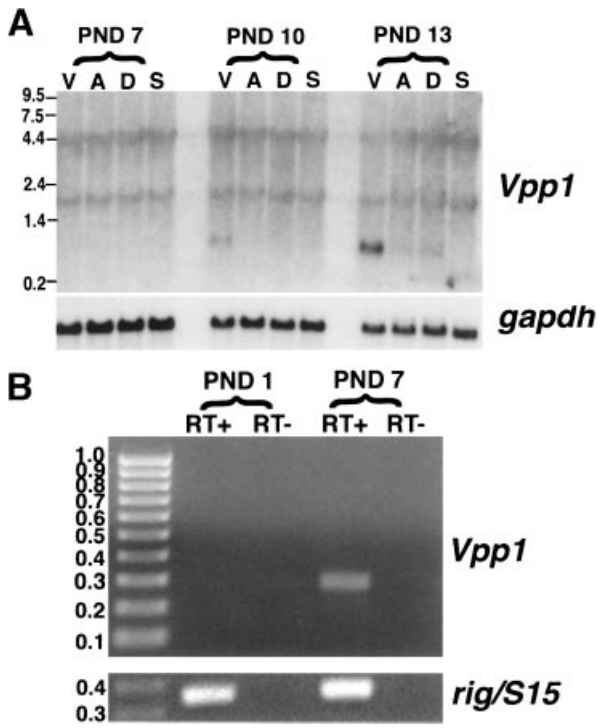


**Fig. 4.** Developmental expression of *Vppl*. **A** (Top): For Northern analysis, total RNA (3 μg/lane) was transferred to a membrane and hybridized with a *Vppl* cDNA probe. Developmental stages were PND7, 10, and 13. **Lanes V**, ventral prostate; **Lanes A**, anterior prostate; **Lanes D**, dorsolateral prostate; **Lanes S**, seminal vesicle. A (Bottom): Hybridization of the same blot with a GAPDH probe. **B**: RT-PCR analysis of *Vppl* expression in PNDI total prostate RNA, and PND7 ventral prostate RNA. RT+, reverse transcription; RT−, no reverse transcription (control); *rig/SI5*, constitutively expressed gene (positive control). The amplified *Vppl* partial cDNA product was 300 bp.

in the ventral lobe during branching morphogenesis and in mature prostate glands. The amino acid sequence encoded by *Vpp1* predicts a 135 amino acid secreted protein.

An extensive survey covering 13 urogenital tissues and 16 non-urogenital tissues demonstrated that *Vpp1* is expressed exclusively in the mouse prostate gland. To our knowledge, *Vpp1* is the only mouse gene reported to date that is not expressed in any tissue other than the prostate gland. Although several human prostate-unique genes have been identified including *PCGEM1* [14], *PSGR* [15], *prostein* [16], and *DD3* [17], no mouse homologs of these genes have been reported. Interestingly, BLAST analysis of *Vpp1* against the human genome database failed to reveal significant homology to any available human sequence. One explanation for the apparent lack of a clear human homolog of *Vpp1* is that the two genes have diverged to the extent that their degree of homology falls below the threshold for detection

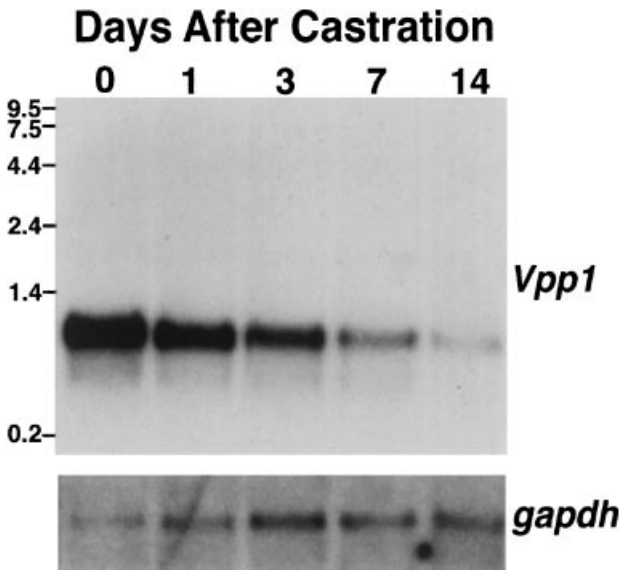


**Fig. 5.** Effect of castration on *Vppl* expression. At each time point after castration, total prostate RNA from two mice was pooled and screened by Northern blot analysis for expression of *Vppl* (top). 0, untreated, day of castration; 1, 1 day post-castration; 3, 3 days post-castration; 7, 7 days post-castration; 14, 14 days post-castration. Hybridization of the same blot with a GAPDH probe (bottom).

by currently available alignment algorithms. Alternatively, a human counterpart of *Vpp1* could reside in any of the reported > 90,000 gaps that average 2.43 kb in length in the deposited human genome sequence

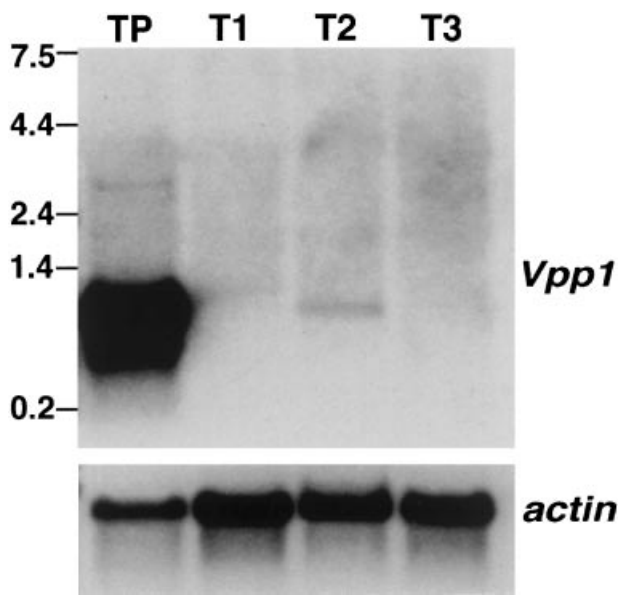


**Fig. 6.** Expression of *Vppl* in prostate tumors. Prostate tumors were dissected from 6–11 month-old TRAMP mice. Total RNA was screened by Northern blot analysis for *Vppl* expression (top). *TP*, total prostate RNA from age-matched normal C57BL/6J mice; T1, tumor #1; T2, tumor #2; T3, tumor #3. Hybridization of the same Northern filter with a β-actin probe (bottom).

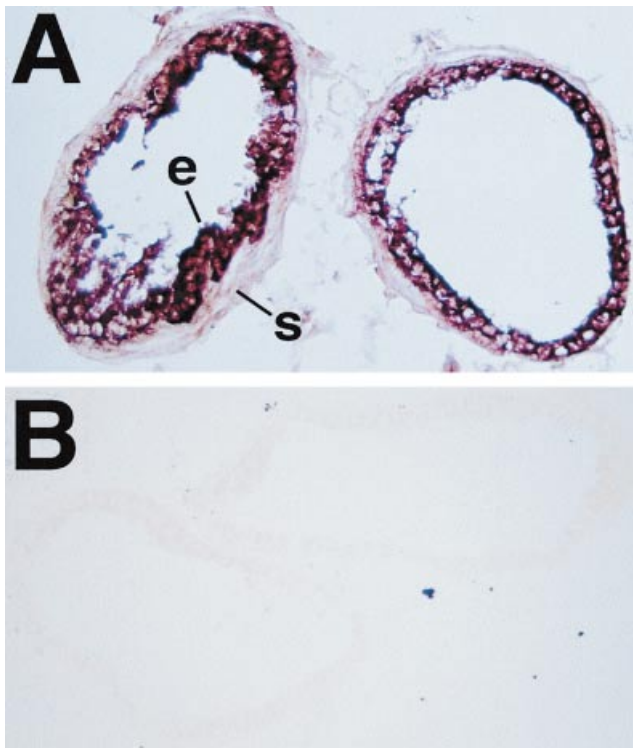


**Fig. 7.** In situ hybridization analysis of *Vppl* expression in adult prostate. **A**: Bright-field photomicrograph of a section of the ventral prostate hybridized with the *Vppl* probe. A strong hybridization signal was confined to ductal structures and found exclusively over epithelial cells. **B**: View of a section adjacent to that of A hybridized with a control probe exposed for the same time and photographed under identical conditions. e, epithelial cells; s, stromal cells.

[18]. The most interesting alternative is that *Vpp1* is a species-specific gene expressed only in the mouse prostate. The biological and biochemical characterization of species-specific genes could play an important role in understanding disparities in prostate biology between rodents and humans, particularly with respect to the clear differences in morphology and disease susceptibility.

The exquisite prostate-specificity of *Vpp1* expression may allow this gene to serve as a paradigm to determine the molecular basis of prostate-specific gene expression. Identification of cis-acting control elements that direct expression of *Vpp1* to the prostate will provide insights into the nature of the transcriptional regulatory complex that mediates its unique expression pattern.

Androgen regulation of gene expression plays a pivotal role in prostate growth and differentiation. During embryogenesis, mesenchymal androgen receptors are required for prostate outgrowth [1], and are essential later in epithelial cells to facilitate differentiation of a full secretory phenotype [19]. The decrease in *Vpp1* mRNA after castration suggests that

maintenance of the steady-state level of the gene requires testicular androgens. A recent BLAST search identified an unpublished cDNA sequence (accession no. AF319955) from an androgen-upregulated transcript selectively expressed in the mouse prostate that is 99% identical to *Vpp1*. These data support our observations of both prostate specificity and androgen regulation of *Vpp1*.

Since a prominent tumor suppressor pathway has not been identified for prostate cancer, most existing animal models have been developed using gain-of-function approaches to express known oncogenes in prostate epithelial cells of transgenic mice. Prominent among these is the TRAMP model, in which the simian virus 40 (SV40) early region is driven by a minimal promoter from the rat probasin gene [20,21]. The SV40 large T and small t antigen oncoproteins interfere with the Rb and p53 proteins, which regulate the two principal tumor suppressor pathways active in most cells. TRAMP mice develop progressive prostate disease beginning with focal adenocarcinomas that metastasize to lymph nodes, lung, and, in the FVB genetic background, skeletal bones [21]. This example and other iterations of the basic model have proven useful in studying certain aspects of prostate cancer including the effects of castration, the role of insulin-like growth factor, and to establish cell lines to test immunotherapies [22–25]. The observation that *Vpp1* mRNA accumulation is extensively down-regulated or extinguished in all of the TRAMP tumors analyzed suggests that expression of this gene, as with other androgen regulated genes [26–28] may be incompatible with the malignant phenotype of prostate epithelial cells.

## CONCLUSIONS

*Vpp1* is a novel mouse gene that is preferentially expressed in the ventral lobe of the prostate gland during the early postnatal period through adulthood. It appears to encode a secreted protein with no recognizable homology to known proteins. The early onset of *Vpp1* transcription in the first week of postnatal life together with the observation that its expression is confined exclusively to the prostate gland is consistent with this gene playing a specific role in prostate growth and/or function. These features may also allow *Vpp1* to serve as a paradigm to elucidate the molecular basis of region-preferred, prostate-unique gene expression.

## REFERENCES


1. Cunha GR, Donjacour AA, Cooke PS, Mee S, Bigsby RM, Higgins SJ, Sugimura Y. The endocrinology and developmental biology of the prostate. Endocr Rev 1987;8:338–363.
2. Sciavolino PJ, Abate-Shen C. Molecular biology of prostate development and prostate cancer. Ann Med 1998;30:357–368.
3. McNeal JE. The prostate gland: morphology and pathobiology. Monogr Urol 1983;4:3–33.
4. McNeal JE. Normal anatomy of the prostate and changes in benign prostatic hypertrophy and carcinoma. Semin Ultrasound, CT MR 1988;9:329–334.
5. Qian J, Bostwick DG. The extent and zonal location of prostatic intraepithelial neoplasia and atypical adenomatous hyperplasia: relationship with carcinoma in radical prostatectomy specimens. Pathol Res Pract 1995;191:860–867.
6. Price D. Comparative aspects of development and structure in the prostate. Natl Cancer Inst Monogr 1968;12:1–12.
7. Waynforth HB. Experimental and surgical techniques in the rat. San Diego, CA: Academic Press, Inc; 1980.
8. Sugimura Y, Cunha GR, Donjacour AA. Morphogenesis of ductal networks in the mouse prostate. Biol Reprod 1986;34: 961–971.
9. Nakai K, Horton P. PSORT: a program for detecting sorting signals in proteins and predicting their subcellular localization. Trends Biochem Sci 1999;24:34–36.
10. Inoue C, Shiga K, Takasawa S, Kitagawa M, Yamamoto H, Okamoto H. Evolutionary conservation of the insulinoma gene rig and its possible function. Proc Natl Acad Sci U S A 1987; 84:6659–6662.
11. Kitagawa M, Takasawa S, Kikuchi N, Itoh T, Teraoka H, Yamamoto H, Okamoto H. Rig encodes ribosomal protein S15; the primary structure of mammalian ribosomal protein S15. FEBS Lett 1991;283:210–214.
12. Komminoth P, Merk FB, Leav I, Wolfe HJ, Roth J. Comparison of 35S- and digoxigenin-labeled RNA and oligonucleotide probes for in situ hybridization. Expression of the seminal vesicle secretion protein II and androgen receptor genes in the rat prostate. Histochemistry 1992;98:217–228.
13. Kozak M. An analysis of 5′-noncoding sequences from 699 vertebrate messenger RNAs. Nucleic Acids Res 1987;15:8125–8148.
14. Srikantan V, Zou Z, Petrovics G, Xu L, Augustus M, Davis L, Livezey JR, Connell T, Sesterhenn IA, Yoshino K, Buzard GS, Mostofi FK, McLeod DG, Moul JW, Srivastava S. *PCGEM*1: a novel prostate specific gene is overexpressed in prostate cancer. Proc Natl Acad Sci U S A 2000;97:12216–12221.
15. Xu LL, Stackhouse BG, Florence K, Zhang W, Shanmugam N, Sesterhenn IA, Zou Z, Srikantan V, Augustus M, Roschke V, Carter K, McLeod DG, Moul JW, Srivastava S. *PSGR*, a novel prostate-specific gene with homology to a G protein-coupled receptor, is overexpressed in prostate cancer. Cancer Res 2000;60:6568–6572.
16. Xu J, Kalos M, Stolk JA, Zasloff EJ, Zhang X, Houghton RL, Filho AM, Nolasco M, Badaro R, Reed SG. Identification and characterization of prostein, a novel prostate-specific protein. Cancer Res 2001;61:1563–1568.
17. Bussemakers MJH, Van Bokhoven A, Verhaegh GW, Smit FP, Karthaus HF, Schalken JA, Debruyne FM, Ru N, Isaacs WB. DD3: a new prostate-specific gene, highly expressed in prostate cancer. Cancer Res 1999;59:5975–5979.
18. Venter JC, Adams MD, Meyers EW, et al. The sequence of the human genome. Science 2001;291:1304–1351.
19. Donjacour AA, Cunha GR. Assessment of prostatic protein secretion in tissue recombinants made of urogenital sinus mesenchyme and urothelium from normal or androgen-insensitive mice. Endocrinology 1993;132:2342–2350.

20. Greenberg NM, DeMayo FJ, Finegold MJ, Medina D, Tilley WD, Aspinall JO, Cunha GR, Donjacour AA, Matusik RJ, Rosen JM. Prostate cancer in a transgenic mouse. Proc Natl Acad Sci U S A 1995;92:3439–344327.
21. Gingrich JR, Barrios RJ, Morton RA, Boyce BF, DeMayo FJ, Finegold MJ, Angelopoulou R, Rosen JM, Greenberg NM. Metastatic prostate cancer in a transgenic mouse. Cancer Res 1996;56:4096–4102.
22. Gingrich JR, Barrios RJ, Kattan MW, Nahm HS, Finegold MJ, Greenberg NM. Androgen-independent prostate cancer progression in the TRAMP model. Cancer Res 1997;57:4687–4691.
23. Kaplan PJ, Mohan S, Cohen P, Foster BA, Greenberg NM. The insulin-like growth factor axis and prostate cancer: lessons from the transgenic adenocarcinoma of mouse prostate (TRAMP) model. Cancer Res 1999;59:2203–2209.
24. Foster BA, Gingrich JR, Kwon ED, Madias C, Greenberg NM. Characterization of prostatic epithelial cell lines derived from transgenic adenocarcinoma of the mouse prostate (TRAMP) model. Cancer Res 1997;57:3325–3330.
25. Kwon ED, Hurwitz AA, Foster BA, Madias C, Feldhaus AL, Greenberg NM, Burg MB, Allison JP. Manipulation of T cell costimulatory and inhibitory signals for immunotherapy of prostate cancer. Proc Natl Acad Sci U S A 1997;94: 8099–8103.
26. Kasper S, Sheppard PC, Yan Y, Pettigrew N, Borowsky AD, Prins GS, Dodd JG, Duckworth ML, Matusik RJ. Development, progression, and androgen-dependence of prostate tumors in probasin-large T antigen transgenic mice: a model for prostate cancer. Lab Invest 1998;78:319–333.
27. Masumori N, Thomas TZ, Chaurand P, Case T, Paul M, Kasper S, Caprioli RM, Tsukamoto T, Shappell SB, Matusik RJ. A probasin-large T antigen transgenic mouse line develops prostate adenocarcinoma and neuroendocrine carcinoma with metastatic potential. Cancer Res 2001;61:2239–2249.
28. Chaurand P, DaGue BB, Ma S, Kasper S, Caprioli RM. Strain-based sequence variations and structure analysis of murine prostate specific spermine binding protein using mass spectrometry. Biochemistry 2001;40:9725–9733.